A "20 T at 20 K" Model Coil for the Muon Collider Target Solenoid and Fusion Applications

Luca Bottura, B. Bordini, M. Catellani, R. Losito, A. Trotta, M. De Bastiani, D. Indrigo, E. De Marchi, E. Gallo, A. Spagnuolo, F. Beggio, C. Luongo, L. Giannini, G. Federici, M. Casciello, M. De Stasio, L. Savoldi, M. Breschi, A. Macchiagodena, L. Cavallucci, A. Portone, and M. Statera

***Abstract*—The development of high-field, large-bore magnets based on High-Temperature Superconductors (HTS) is a strategic challenge with impact across high-energy physics, fusion energy, and other scientific and societal applications. In particular, the target decay and capture solenoid for the Muon Collider and the central solenoid of next-generation fusion devices both demand solenoids capable of producing a 20 T peak field in a bore larger than 1 m, at 20 K, with stored energy exceeding 300 MJ (single coil). Such performance is well beyond present state-of-the-art, requiring a dedicated programme to validate conductor technologies, magnet architectures, and protection strategies. This paper presents the results of a feasibility study originated from discussions between CERN and Eni on a common solenoid concept serving as technology validation for both high-energy physics experiments and magnetic-confinement fusion devices such as tokamaks. The main result of the study, which brought together universities and research centers, is a "20@20" model coil concept. We report here the rationale for the selection of the target performance of the "20@20" model coil, and the highlights of the study, which was instrumental to identify high priority developments required towards its realization.**

***Index Terms*—High-temperature superconductors, HTS, model coil, Muon Collider, magnetically confined fusion.**

I. Introduction

HIGH-FIELD and large bore magnets are critical for advancing applications in particle accelerators [1], fusion research [2], life and materials science in high field [3]. Bore fields in excess 20 T over a large free bore, 1 m diameter and larger, were identified as targets that are fully relevant to the next step in magnet technology for the above fields of scientific and societal applications. These performance targets are well beyond present state-of-the-art and can only be produced by resorting to High-Temperature Superconductors (HTS), in particular REBCO (rare-earth barium copper oxide) tapes. REBCO offers the additional benefit of operation at higher cryogenic temperatures compared to low-temperature superconductors (LTS), e.g., enabling operation at around 20 K rather than 1.9 K to 4.2 K. This decreases considerably the power needed to run the cryo-plant, and higher stability margins may allow for coil pack designs incorporating indirect cooling. Thus, HTS not only has potential to extend the magnetic field reach, but also makes applications possible that were not within a practical or affordable range with other superconductors.

CERN and Eni have recognized the immediate need of a dedicated programme to validate conductor technologies, magnet architecture, and protection strategy, and have joined forces to propose a model coil as the catalyzer of efforts and cross-sector demonstrator. The design, construction, and testing of the model coil will enable Technology Readiness Level (TRL) progression while also establishing a robust framework for industrial scalability, reliability, and maintainability. This initiative may serve multiple communities by providing open validation data and fostering the industrial supply chain capable of producing reactor-grade HTS magnet systems. The program will act as a shared platform to de-risk key technologies, bridge the requirements of accelerators and fusion reactors, and accelerate the transition to deployable, long-life HTS magnet systems. Last not least, a model coil with field reach in the range of 20 T, properly fitted, will serve as background field for a future test facility largely out-performing present capability. Such value proposition has elicited interest beyond the initial scope of bilateral collaboration, presently expanded to include the other institutions that have actively contributed to the feasibility study reported here.

To set performance targets for the model coil, we began scrutinizing the requirements of the Target, Decay and Capture Solenoid of the Muon Collider, defined in [4], [5], and those of the Central Solenoid (CS) of high field, compact tokamaks (HFCT, e.g., ARC Class Object) as defined in [6]. The result of this exercise is shown in Table I and Fig. 1, where we report numerically and graphically the most relevant magnet design parameters and operating conditions of the two types of applications, which we refer to as "performance metrics". Demonstrating field strength and bore is not sufficient for a magnet system to be viable in any application. Successful

Received 5 September 2025; revised 14 November 2025; accepted 3 December 2025. Date of publication 10 February 2026; date of current version 13 February 2026. This work was supported in part by the European Union (EU). *(Corresponding author: Luca Bottura.)*

Luca Bottura, B. Bordini, M. Catellani, and R. Losito are with the CERN, 1217 Geneva, Switzerland (e-mail: luca.bottura@cern.ch).

A. Trotta, M. De Bastiani, D. Indrigo, E. De Marchi, E. Gallo, A. Spagnuolo, and F. Beggio are with the ENI, 00144 Rome, Italy.

C. Luongo, L. Giannini, and G. Federici are with the EUROFusion, 85748 Garching, Germany.

M. Casciello, M. De Stasio, and L. Savoldi are with the Politecnico di Torino, 10129 Torino, Italy.

M. Breschi, A. Macchiagodena, and L. Cavallucci are with the Universita' di Bologna, 40126 Bologna, Italy.

A. Portone is with the Fusion for Energy (F4E), 08019 Barcelona, Spain.

M. Statera is with the INFN, 00186 Milano, Italy.

Color versions of one or more figures in this article are available at https://doi.org/10.1109/TASC.2026.3656861.

Digital Object Identifier 10.1109/TASC.2026.3656861

TABLE I
KEY PERFORMANCE INDICATORS FOR HTS SOLENOIDS APPLICATIONS FOR FUSION AND HIGH ENERGY PHISICS, AND TENTATIVE PARAMETER SET FOR THE ENGINEERING DESIGN OF A HTS MODEL COIL

Performance metric	HFCT – ARC-like Central Solenoid	Muon Collider Target solenoid	20@20 Model Coil
Peak Magnetic Field	20 T	20 T	20 T
Coil free bore	1 m	1.4 m	1 m
Stored magnetic energy (system/coil)	5 GJ / 800 MJ	1.5 GJ / 300 MJ	- / 550 MJ
Operating temperature	15 K ... 20 K	20 K (15 K ... 25 K)	20 K (15 K...25 K)
Operating Current	35 kA	60 kA	61 kA
Operating Voltage	+/- 2.5 kV	+/- 2.5 kV	+/- 2.5 kV
Operating Stress (von Mises)	700 MPa	700 MPa	700 MPa
Ramp up time	100 s	< 1 hour	100 s
Flat-top	1800s	> 12 h	> 12 h
Ramp down time	100s	< 1 hour	100 s
Heat load per unit conductor length	2 ... 4 W/m	2 W/m	2 ... 4 W/m
Number of Powering cycles	>40000	>1000	>1000
Number of Thermal cycles	>50	>50	> 50
Radiation dose/DPA		80 MGy/10^{-3}	-
Expected lifetime	20 y	20 y	20 y

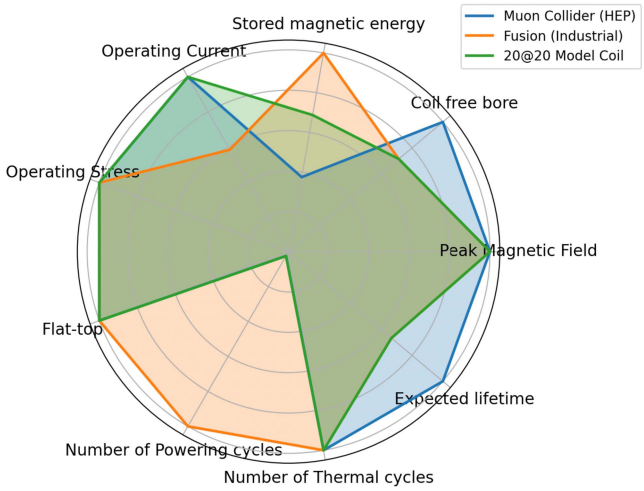

Fig. 1. Polar plot of selected magnet design requirements for the Target, Decay and Capture solenoid of a Muon Collider, and the Central Solenoid (CS) of high field, compact tokamaks (data from Table I). For comparison, we report the design target of the 20@20 model coil.

deployment and exploitation require a comprehensive strategy encompassing reliability, maintainability, and lifecycle assessment. This is particularly true for fusion reactors, demanding continuous operation, predictive maintenance, and decades-long asset integrity.

Parameters such as Mean Time Between Failures (MTBF), Mean Time To Repair (MTTR), accessibility for maintenance, monitoring and diagnostics coverage will need to be evaluated. Such evaluation goes beyond the scope of the conceptual design study reported here, but will be integral part of the Asset Integrity Management (AIM) of the model coil programme proposed.

The metrics for HEP and fusion applications have a wide overlap of characteristics, which profits the selection of targets for a model coil serving both communities. But there are also a few requirements that differ and deserve commenting. The first is the ramp and flat-top time, whereby the solenoids of a tokamak need to be swept rapidly to provide a flux swing and contribute to plasma equilibrium, while a particle capture solenoid operates in steady state. A direct consequence is the large difference in the number of powering cycles, and associated fatigue. Finally, the particle target for HEP applications is typically a high radiation area, with large dose and DPA scores, while fusion solenoids tend to be well shielded and receive significantly less dose. It is worth noting that heat loads, on the other hand, do not differ much, though they are from different origin: mainly AC loss for fusion application, and of nuclear nature for HEP.

We report in last column of Table I a first set of design targets for the model coil. A graphical impression of the area of parameters covered by the model coil is also reported in Fig. 1. The logic followed was to cover as much as possible of the overlapping parameter space, subject to the optimization, feasibility and cost considerations discussed later. While we included the ability of fast ramping, crucial to fusion applications and beneficial for HEP, we have not retained the large number of cycles, nor the radiation dose and DPA among the targets. Indeed, material fatigue and radiation effects are issues that can be addressed more effectively by parallel programs on material and conductor samples, while fatigue testing of the model coil would imply unreasonable effort, and radiation testing is in practice impossible.

In summary, a solenoid model coil capable of producing 20 T in a bore of about 1 m, storing approximately 550 MJ of magnetic energy, and operating stably at 20 K emerges as the ideal demonstrator to validate key performance targets and de-risk critical technologies [7]. This is the "20@20 model coil" described in this paper. Achieving this performance is a significant challenge, at the forefront of magnet science and technology. Several teams are active worldwide in the development and demonstration of high field HTS magnets, a sample and non-exhaustive list is provided in references [8], [9], [10], [11]. Still, to date no HTS coil of size and performance matching the targets of the 20@20 model coil has been built and successfully tested.

We report in the following sections highlights from the feasibility study performed to explore suitable design configurations of solenoids meeting the target performance, identify the main challenges, and evaluate whether they can be addressed through targeted engineering analyses and R&D. The main outcome of the study is that a 20@20 model coil within the targeted parameter space appears to be feasible. We emphasize that this is not yet a full design description. The mandatory detailed engineering design and technology development will follow.

II. Key Challenges

Reaching the target field of 20 T in a 1 m bore solenoid operating at 20 K is ambitious. Below we report the main perceived challenges, also including the perspective of long-term industrial applicability.

Superconductor material performance, cost and supply chain. HTS tapes provide high engineering current density at 20 K, but with the present production capability and yield their cost and availability remain limiting factors. It is hence essential to maximize magnetic efficiency to reduce conductor mass, while also addressing industrial variability. On the procurement side, a multi-vendor strategy, standardization and robust QA are key to qualify and secure suppliers, and ensure scalability.

High Lorentz forces and structural integrity. At 20 T, sheer magnetic pressure reaches 160 MPa, and the actual stress is amplified by structural material dilution and peaks in the distribution. The mechanics of a large bore 20 T solenoid is therefore one of the limiting design factors to be considered in the design process from the outset. Besides structural integrity, the engineering design will need to integrate allowance for inspection, monitoring and maintainability.

Quench detection, protection and recovery. With stored energy of 300 MJ and larger, quench protection is a critical engineering, safety and cost challenge. Protection strategies must combine robust detection with safe energy dump, considering practical voltage limits compatible with insulation or no-insulation technology, as applicable. A robust quench management system is crucial to mitigate operational risks, and prevent degradation.

Cryogenic cooling and operational resilience. Operation at 20 K is not a simple extrapolation of cooling with liquid or dense supercritical helium, between 4.2 K and 4.5 K. It requires appropriate selection of operating conditions to provide the desired heat removal capability, with the necessary steady-state and transient operating margins, while achieving high thermodynamic efficiency. Gas cooling at 20 K for a large-scale application is likely to require the development of dedicated refrigerator technology, with low maintenance and suitable redundancy to ensure high reliability.

Heat loads and operational efficiency. HTS tapes and cables exhibit higher AC losses than multi-filamentary LTS wires and cables, increasing cryogenic demand. This not only affects efficiency but also long-term operational costs. Advanced cable concepts, monitoring through digital twins, and predictive operation strategies will be key to controlling AC loss and optimizing performance.

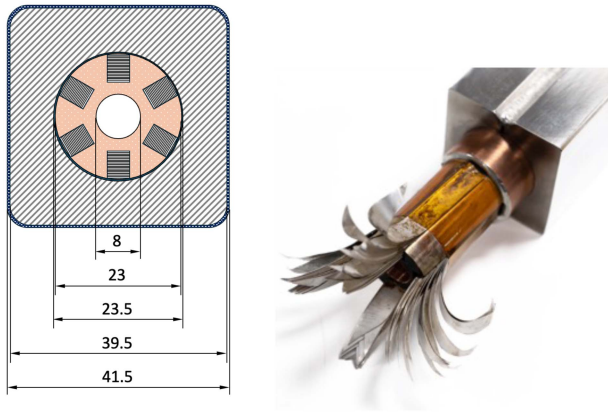

Fig. 2. On the left a cross-section of the baseline conductor (dimensions in mm) and on the right a picture of a conductor mockup built at CERN.

TABLE II
REBCO Tape Geometry and Performance

Substrate thickness	(μm)	40
REBCO thickness	(μm)	2
Copper thickness (total)	(μm)	20
Tape thickness	(μm)	62
Tape width	(mm)	4
J_C^{eng} (20 T, 20 K)	(A/mm^2)	933

Manufacturing, QA/QC and lifecycle considerations. The feasibility of such magnets ultimately depends on industrial-scale manufacturing with QA/QC, traceability, and acceptance testing. From the outset, asset integrity management, lifetime modelling, and maintainability must be part of the design strategy to ensure that the system remains reliable in fusion reactors or collider facilities.

III. Conductor Design

The baseline forced-flow internally cooled conductor concept that we have selected for this study, shown in Fig. 2, is a variant of the one reported in [5], derived from the VIPER and PIT–VIPER designs developed by MIT and CFS, and is designed for an operating point of 20 T at 20 K [12], [13]. It targets a high operating current (30–60 kA) to limit inductance and voltage during operation and quench, uses industrially available REBCO tapes, and incorporates a stainless–steel jacket to withstand electromagnetic loads. The copper current density is kept below 200 A/mm^2 to facilitate standard quench detection and energy extraction. The choice of this design was motivated by considerations of validated performance with minimal degradation [12], priming technology readiness and industrial scalability.

Tables II and III report the tape and conductor characteristics assumed for the design, the expected performance and margins. As reported there, two design variants were evaluated. The nominal design is based on using 80 REBCO tapes per stack, and meets all performance targets at 62 kA, 20 T, and 20 K with a comfortable operating margin of nearly 10 K. Its main limitation lies in the large tape demand, translating into high costs at today's REBCO price levels. A cost–limited variant was

TABLE III
HTS CONDUCTOR GEOMETRY, EXPECTED PERFORMANCE AND MARGINS

		Nominal	Cost-limited
HTS stack width	(mm)	4	
HTS stack thickness	(mm)	5	
HTS tapes/stack	(-)	80	46
Number of HTS stacks	(-)	6	
Operating current	(kA)	62	
Operating field	(T)	20	
Operating temperature	(K)	20	
Critical current	(kA)	112	64
Temperature margin	(K)	9.5	0.5
J^{eng}	(A/mm^2)	36	

considered, reducing the stack to 46 tapes, while preserving the same external geometry with fillers. This approach halves the tape cost but leaves only 0.5 K margin, effectively operating at critical current. While more economical, this narrow margin may impact quench limits and could be impractical if tape uniformity is insufficient. A benefit of the conductor configuration selected is the flexibility that can be achieved modulating the number of HTS and filler tapes in a stack. We plan to use this degree of freedom to adjust performance vs. cost, while also coping with the longitudinal and batch-to-batch variability of critical current inherent with present industrial production of REBCO. The final design, in particular the number of tapes, will be set during the engineering design and validation phase, as a function of test results on full-size samples.

IV. ELECTROMAGNETIC OPTIMIZATION

The design of the model coil was initiated through an optimization of geometry and operating conditions to meet the performance targets of Table I while minimizing the conductor usage and cost. An initial evaluation assumed a homogeneous engineering current density of 50 A/mm^2, higher than the baseline conductor value of 36 A/mm^2 from Table III. The reason for this choice was to meet the stress target, as we obtain requiring that the single-turn stress, JBR, matches the value of 700 MPa from Table I, for a bore radius of 0.7 m and a central field of 20 T. Subsequent optimization steps, reported later, adjusted the geometry to account for the lower current density of the insulated reference conductor, and the use of a finite number of turns and pancakes.

In a first optimization exercise we have set a 20 T field objective and scanned the coil bore and height to minimize the conductor length (see Fig. 3). Reducing the solenoid size proved advantageous: for a 0.5 m bore radius (1 m inner diameter), the minimum conductor length (approximately 3 km) occurs at coil heights larger then 1.2 m, whereas increasing the bore radius to 0.7 m raises the conductor length requirement by over 60% (approximately 5 km). Accordingly, 0.5 m bore radius was selected as the reference. Larger coil heights were also beneficial, lowering the peak-to-central field ratio and stored energy (see Fig. 4). At 1.4 m height, for example, the peak field reaches only 22 T, about 10% above the central field. Based on these considerations, a 1.4 m coil height was adopted as the

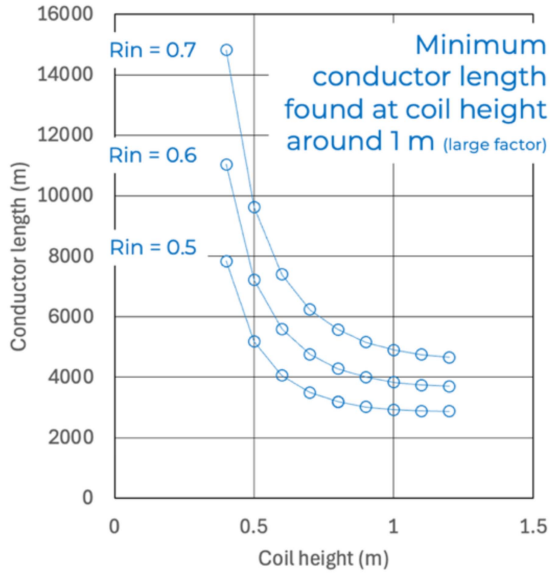

Fig. 3. Conductor length required to wind a solenoid that produces 20 T in the center, as a function of the coil height, taking the inner radius of the solenoid as a parameter.

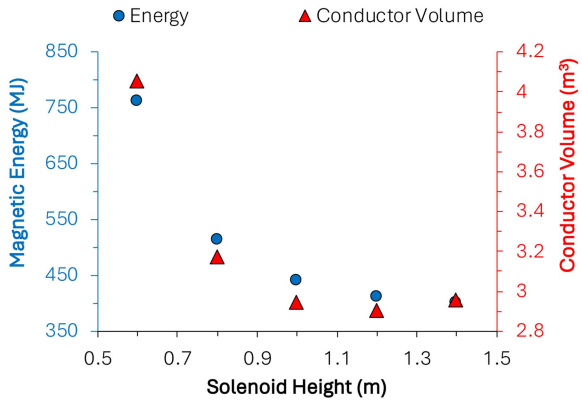

Fig. 4. Stored magnetic energy and total conductor mass in a solenoid of 0.5 m bore radius that produces 20 T in the center, as a function of the coil height, under the assumption of 50 A/mm^2 current density.

reference geometry. The resulting field map for this reference configuration (0.5 m bore radius, 1.4 m height, 50 A/mm^2 current density) is shown in Fig. 5.

A second optimization study targeted a minimum stored energy of 300 MJ using a parametric design and optimization tool that besides geometric and electromagnetic parameters, also considered structural and protection limits. The range of feasible designs was narrow but well defined, with an optimum found for inner radius in the range 0.45 m to 0.5 m, coil height in the range 1.3 m to 1.4 m, and a coil height-to-thickness ratio of about 2.5 [14]. It is worth noting that both optimization approaches converged on similar dimensions, lending robustness to the selection of the reference geometry.

The final step in the electro-magnetic design incorporated conductor discretization, based on the reference geometry of Fig. 2, as well as the presence of inter-turn, inter-pancake, and ground insulation layers. The final geometry is reported in Fig. 6

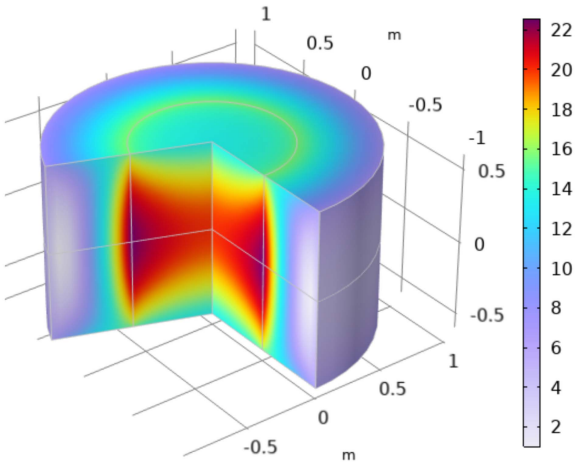

Fig. 5. Model coil configuration under the assumption of 50 A/mm^2 current density, inner bore of 0.5 m radius and height of 1.4 m.

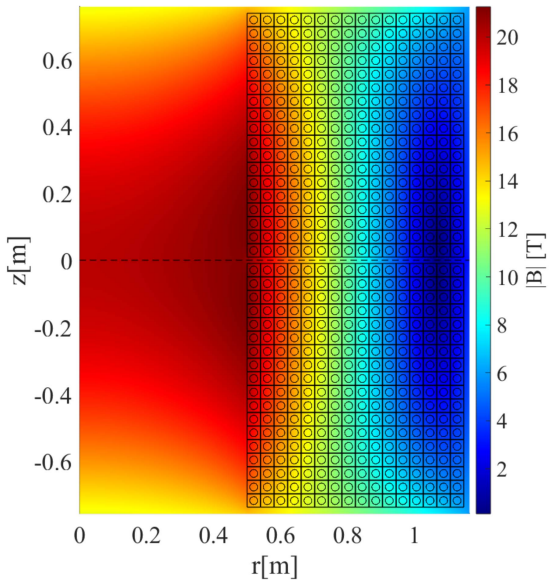

Fig. 6. Initial configuration for the model coil under the assumption of 50 A/mm2 current density, inner bore of 0.5 m radius and height of 1.4 m.

and consists of two identical modules of 1 m bore diameter, each 747 mm in height and 664 mm in thickness. Each module contains 18 pancakes of 16 turns each, enabling the full coil to reach a peak field on-axis of 20.2 T at the nominal operating current of 62 kA, slightly exceeding the target. Under these conditions, the peak field on the conductor is 21.0 T, the total inductance is 285.5 mH and the stored energy 550 MJ. A single module operating at nominal current achieves 12.7 T on-axis, and 15.5 T on the conductor, highlighting the relevance of testing individual modules as an advantageous preparatory step toward the full model coil.

V. Mechanics

The coil design is based on a double pancake winding, with standard insulation (glass fiber and resin impregnation). The conductor jacket acts as the primary structural element to withstand all forces. This is once more a well-established concept,

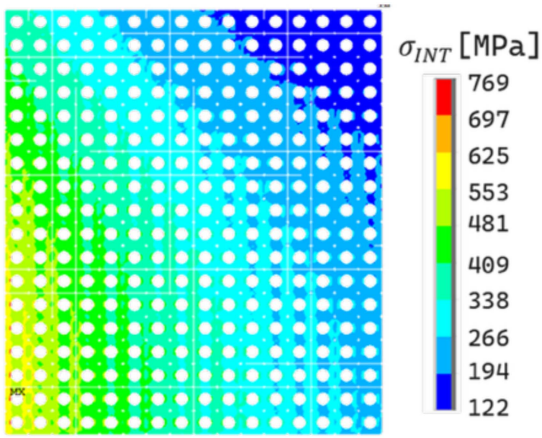

Fig. 7. Stress intensity in the conductor jackets under the nominal Lorentz load. Only one module (half of the full magnet) is shown; the stress distribution in the second module is, of course, symmetric.

with high technology readiness. A preliminary mechanical feasibility analysis has been carried out on the proposed 20@20 model coil design using a 2D axisymmetric finite element model developed in Ansys APDL [15]. To keep the computational cost of the global model reasonable, the details of the cable have been omitted (see later discussion), substituted by a copper core with cooling hole in which the overall integral force of the cable is uniformly distributed in the cross section. In such a way the overall effect on the jacket and insulation is preserved. Material properties and limits were based on the ITER design code [16], which provides a generally accepted and traceable reference. So far, the only load case considered is the electromagnetic force. The static assessment under nominal load confirmed the structural integrity of both the conductor jacket and cable insulation. As illustrated in Fig. 7, the highest stress intensities arise in the innermost turns of the equatorial plane, reaching the desired range of 700 MPa. The structural safety factor remains above unity across all conductor jackets. Localized regions of high stress were identified in the insulation, but these can be mitigated through minor design refinements. Fatigue effects have not been considered, also given the relatively low number of powering (1000) and thermal (50) cycles targeted. Nonetheless, we plan dedicated analyses in future design phases to evaluate performance under cyclic loading.

Similar to what done in [5], a detailed analysis of the most stressed turn was also performed to assess the stress state in the superconducting tapes and its potential impact on critical current degradation. The conductor was meshed to the single tape level, including features such as internal spacers and solder filling. The displacement of the jacket external surface of the more stressed turn was imported from the global coil model, and used as boundary condition in the single conductor model, while the electromagnetic force was distributed evenly in the tape stacks, corresponding to an assumption of uniform current distribution. This model provides the multiaxial stress state in the HTS tapes under nominal load conditions.

An issue in the evaluation of the results is that while irreversible critical current degradation of REBCO conductors under uniaxial strain and stress is relatively well established. a

direct quantitative correlation of the effect of multiaxial stress states on critical current is not available. To by-pass this issue, we have used the published results of transverse compression testing on the PIT–VIPER cable developed by CFS [13] as a benchmark. A model of the PIT-VIPER cable was built with resolution similar to the one used for the 20@20 conductor, and the stress state was computed for the conditions that correspond to the onset of critical current degradation, i.e., 600 MPa from [13]. The local stress levels predicted in the 20@20 model coil at nominal operation were found to be significantly lower than those associated with onset of permanent degradation in the CFS experiments, suggesting that the nominal operating loads on the conductor in the 20@20 model coil should not compromise cable performance.

To further de–risk the design, dedicated experimental campaigns are envisage in the next project phase, including HTS material characterization in the relevant temperature range, mechanical performance testing of the cable (minimum bending radius, tape twist effects), stress thresholds for permanent tape degradation, insulation electrical performance under representative Lorentz loads, and optimization of the soldering strategy for the tape stack.

VI. Heat Loads and Cooling

The static heat load evaluation considered contributions from support structures, radiation, instrumentation, current leads, and joints/terminations. At this early stage many details remain undefined, but the dominant contributions are expected to come from HTS current leads (approximately 120 W), inter-pancake joints and terminations (approximately 360 W assuming 5 nΩ resistance), and AC loss during ramps.

AC loss calculations were estimated from hysteresis and coupling losses using analytical models. Coupling losses between tape stacks were evaluated using the Single Time Constant Model (STCM) [17], [18], [19], with nτ = 300 ms obtained from PIT–VIPER conductor data [13]. Hysteresis losses were estimated with a slab-approximation-based method accounting for conductor twist geometry. Calculations were performed for a 0–62 kA current ramp over 100 s at 20 K, both for a full magnet (two modules) and for a single standalone module.

Results show that hysteresis dominates the loss budget: total magnet energy dissipation for a 100 s ramp is 1039 kJ, of which 777 kJ arises from hysteresis and 262 kJ from coupling. Peak hysteresis power reaches 8.7 kW at t = 60 s, with a distribution peaking in the inner turns of a pancake, while coupling losses reaches a 2.6 kW plateau at t = 2 s, with highest value in the inner turn of a pancake. The highest losses occur near the magnet midplane. Analysis indicates that if the conductor lacks resistive barriers, nτ could rise to several seconds, increasing coupling loss energy by up to a factor of 20, exceeding hysteresis losses. Reducing the ramp rate by half would decrease peak coupling loss power by a factor of four and total coupling energy by a factor of two. Given uncertainties in conductor loss properties, dedicated experimental campaigns are recommended to measure hysteresis and coupling losses (including inter-tape currents) prior to magnet winding, across relevant fields, currents, and frequencies.

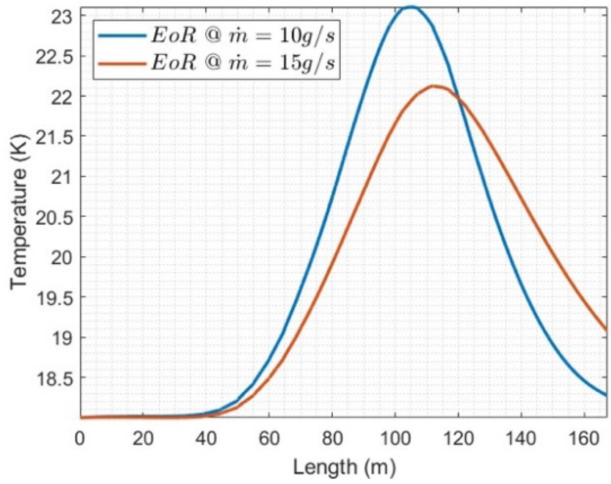

Fig. 8. Temperature distribution along the length at the end of current ramp, with a mass flow of 10g/s(blue line) and 15g/s(orange line) and an initial temperature of 18K, with nτ = 300ms, for a single module.

The cooling layout of each solenoid module is based on double pancakes hydraulically connected in parallel, with helium gas entering at the outer radius of one pancake and exiting at the corresponding radius of the adjacent one. Helium is supplied at 20 bar with an inlet temperature between 15 K and 20 K. The rationale for the selection of these operating conditions are detailed in [5]. A simplified advection–conduction model was implemented to evaluate intra–, inter–layer, and inter–pancake thermal contacts, revealing that the error of assuming an adiabatic cable is < 1 %. Consequently, the adiabatic assumption was adopted for all transient ramp–up analyses in OPENSC2 [20], with thermal loads derived from AC loss calculations.

The temperature profile along the cable is presented in Fig. 8 for helium mass flow rates of 10 g/s and 15 g/s at an initial temperature of 18 K (nτ = 300 ms). Peak temperatures reach 23.1 K for 10 g/s and 22.3 K for 15 g/s, confirming that increased mass flow improves heat removal.

Sensitivity analyses were performed on both single– and full–module configurations. For a single module, a mass flow rate of 15 g/s at 15 K yields a thermal margin of approximately 8 K, while reducing the flow to 10 g/s decreases the margin to about 4 K. In the full–module configuration, critical energy deposition limits are exceeded because of the higher peak magnetic field (20 T) and increased AC losses. The maximum energy the system can sustain corresponds to 60 % of the nominal power, highlighting the need for strategies to reduce AC losses during rapid current ramps. A variable ramp rate strategy—initially fast and then slower near full current— emerges as a promising approach to improve thermal margins and reduce total losses, though further dedicated simulations are required to evaluate this trade–off.

VII. Quench Protection

Quench protection strategies established for low-temperature superconductors (LTS, e.g., NbTi, Nb_3Sn) are not necessarily applicable to HTS/REBCO, due to fundamental differences

TABLE IV
SUMMARY OF DETECTION TIME AND PEAK TEMPERATURES FOR A QUENCH OVER A 5 CM INITIAL NORMAL ZONE, LOCATED IN THE CENTER OF A DOUBLE PANCAKE

Detection Threshold (mV)	Detection time (s)	Temperature at detection time (K)	Maximum temperature (K)
100	9.2	75	86
200	10.2	92	104
500	11.4	106	137

in their thermal and electrical behavior. While HTS conductors benefit from larger intrinsic stability, the observed slow quench propagation fundamentally challenges traditional protection schemes. Quench origins in HTS magnets are also likely to be very different from their LTS counterpart. We expect localized heating (nuclear, AC loss), conductor degradation, or loss of coolant to lead to relatively slow quench initiation, eventually cascading into a thermal runaway. At this stage of the conceptual design, based on the results in [5], we postulate nonetheless that a voltage-based quench detection and an energy dump on an external resistor will be sufficient to protect the model coil. We take values of the detection voltage thresholds in the range of 100 mV to 500 mV, and a maximum terminal voltage of 5 kV for the energy dump, corresponding to a maximum a voltage to ground of ± 2.5 kV. These are values that correspond to standard detection and voltage withstand for large scale superconducting coils.

A preliminary study of quench detection and protection was performed considering a single double pancake and focusing on the initiation and development of a normal zone at the center of the double pancake, where the magnetic field is highest. The method followed is similar to the one outlined in [5] and is based on a 1D model of the developed conductor length. The components in the cable (tapes, copper, solder) are assumed to have the same temperature, while helium and jacket are modeled as separate components at different temperature. Compressible helium flow is considered in the simulations.

Quench is conveniently initiated by a heat input just above the stability margin, over a short length of 5 cm. Quench propagation is, as expected, slow (a few cm/s), and a significant voltage develops only after a few seconds from the quench. Depending on the threshold, more than 9 s (100 mV) to up to nearly 12 s (500 mV) are necessary to reach the voltage threshold. Once the quench is detected and the dump resistor is switched in the circuit, the current drops with a relatively small time constant of 3.5 s. A summary of the values obtained are reported in Table IV. Peak temperatures are in the range of 90 K to 140 K, i.e., a range where differential thermal expansion of metallic components is modest, below 0.1%. This is considered a safe range in LTS magnets built with internally cooled cables, but remains to be confirmed for HTS conductors of VIPER-like architecture. We are in particular concerned by the stress arising from the transverse and longitudinal temperature differential within the conductor, as well as between quenched and unquenched pancakes. We plan in the next future to address this issue with a mechanical analysis based on the model of the single conductor described earlier.

These findings highlight both the feasibility and the challenges of quench protection in HTS coils. The detection times are long due to the intrinsically slow propagation, and the safe-temperature limit for REBCO remains under debate. Still, the above result suggests that a simple "detect and dump" quench protection strategy based on a voltage threshold may be sufficient.

VIII. CONCLUSION

This study originated from discussions between CERN and Eni on the opportunity of developing a common solenoid validation program, serving both high-energy physics experiments and magnetic-confinement fusion devices such as tokamaks. Building on this vision, the present work brought together universities and research centers to jointly address the scientific and technological challenges of HTS common solenoid operating at 20 T and 20 K.

The main result of the study is the indication that a 20 T HTS model coil operating at 20 K seems to be technically achievable using current REBCO tape technology combined with robust mechanical reinforcement and a dedicated helium gas cooling system. The study allowed to identify key challenges to be addressed as a priority: the development of an advanced HTS conductor, maintaining structural integrity under high Lorentz forces, reducing AC losses during ramping, and ensuring a reliable quench detection strategy. The final objective, manufacturing and testing of the 20@20 model coil, is in fact the ideal catalyzer for a staged programme that will begin with the development and thorough characterization of the specific HTS conductor, with suitable electro-mechanical and AC loss properties, will progress through winding tests and validation tests at liquid nitrogen temperature, demonstrating industrial readiness, and finally reach completion with the manufacturing and testing of the two modules of the 20@20 model coil, whereby partial test of the single modules can be envisaged as natural step-up and risk mitigation strategy. Such programme, presently in the detailed definition phase, will profit from synergies and existing experience in companion programmes, and will provide ample scope for the development of industrial QA, a stable supply chain, robust risk management, and overall asset integrity. We plan to integrate the above items as we move towards the engineering design of the model coil with the basic design parameters outlined in this paper.

ACKNOWLEDGMENT

Views and opinions expressed are however those of the author(s) only and do not necessarily reflect those of the EU or European Research Executive Agency (REA). Neither the EU nor the REA can be held responsible for them.

REFERENCES

[1] L. Bottura, S. Prestemon, L. Rossi, and A.V. Zlobin, "Superconducting magnets and technologies for future colliders," *Front. Phys.*, vol. 10, pp. 01–26, 2022, doi: 10.3389/fphy.2022.935196.

[2] X. Li et al., "REBCO coated conductors: Enabling the next generation of tokamak reactors," *Supercond. Sci. Technol.*, vol. 38, 2025, Art. no. 033001.

[3] National Academies of Sciences, Engineering, and Medicine, *The Current Status and Future Direction of High-Magnetic-Field Science and Technology in the United States*. Washington, DC, USA: The National Academies Press, 2024, doi: 10.17226/27830.

[4] C. Accettura et al., "Conceptual design of a target and capture channel for a Muon Collider," *IEEE Trans. Appl. Supercond.*, vol. 34, no. 5, Aug. 2024, Art. no. 4101705.

[5] L. Bottura et al., "Design and analysis of an HTS internally cooled cable for the Muon Collider target and capture solenoid magnets," *Cryogenics*, vol. 144, 2024, Art. no. 103972.

[6] B. N. Sorbom et al., "ARC: A compact, high-field, fusion nuclear science facility and demonstration power plant with demountable magnets," *Fusion Eng. Des.*, vol. 100, pp. 378–405, 2015, doi: 10.1016/j.fusengdes.2015.07.008.

[7] L. Bottura et al., "Magnet R&D for the Muon Collider—european strategy input," European Strategy Group, Tech. Rep. CERN EDMS 3231359, Geneva, Mar. 2025.

[8] Z. S. Hartwig et al., "The SPARC toroidal field model coil program," *IEEE Trans. Appl. Supercond.*, vol. 34, no. 2, Mar. 2024, Art. no. 0600316, doi: 10.1109/TASC.2023.3332613.

[9] J. Lion et al., "Stellaris: A high-field quasi-isodynamic stellarator for a prototypical fusion power plant," *Fus. Eng. Des.*, vol. 214, May 2025, Art. no. 114868, doi: 10.1016/j.fusengdes.2025.114868.

[10] V. Corato et al., "The DEMO magnet system – Status and future challenges," *Fusion Eng. Des.*, vol. 174, Jan. 2022, Art. no. 112971, doi: 10.1016/j.fusengdes.2021.112971.

[11] J. Zheng, "HTS fusion technology status in China," Presentation at CCA-2025, Mar. 2025. [Online]. Available: https://indico.cern.ch/event/1347361/contributions/6308966/

[12] Z. S Hartwig et al., "VIPER: An industrially scalable high-current high-temperature superconductor cable," *Supercond. Sci. Technol.*, vol. 33, 2020, Art. no. 11LT01, doi: 10.1088/1361-6668/abb8c0.

[13] C. Sanabria et al., "Development of a high current density, high temperature superconducting cable for pulsed magnets," *Supercond. Sci. Technol.*, vol. 37, 2024, Art. no. 115010, doi: 10.1088/1361-6668/ad7efc.

[14] L. Giannini, "A European phased R&D program for quench protection of large-scale HTS magnets," Presented at MT-29, Boston, MA, USA, unpublished, 2025.

[15] "Ansys Mechanical APDL command reference," Release 2025 R1, Ansys, Inc., Canonsburg, PA, USA, Jan. 2025.

[16] ITER TF Coil Design Description Document, ITER_D_E4Y698 - DDD11-2, unpublished. [Online]. Available: https://user.iter.org/?uid=E4Y698

[17] M. N. Wilson, *Superconducting Magnets*. London, U. K.: Oxford Univ. Press, 1983.

[18] M. Breschi et al., "AC losses in the first ITER CS module tests: Experimental results and comparison to analytical models," *IEEE Trans. Appl. Supercond.*, vol. 31, no. 5, Aug. 2021, Art. no. 5900905.

[19] M. Breschi et al., "AC losses in the second module of the ITER Central Solenoid," *IEEE Trans. Appl. Supercond.*, vol. 32, no. 6, Sep. 2022, Art. no. 4700505.

[20] L. Savoldi, D. Placido, and S. Viarengo, "Thermal-hydraulic analysis of superconducting cables for energy applications with a novel open object-oriented software: OPENSC2," *Cryogenics*, vol. 124, 2022, Art. no. 103457.